

E. J. Meijer and D. Frenkel, Amsterdam/The Netherlands*

Structure and Phase Equilibria of Colloid-Polymer Mixtures

A Computer Simulation Study

We present a computer simulation study of a simple model for a colloid dispersed in a dilute polymer solution. We use a recently introduced computational scheme that allows direct numerical simulation at constant osmotic pressure of the polymers. We compute the polymer-induced interaction, the local structure of the colloid and the phase diagram. In particular we studied the effect of the non-pairwise additivity of the polymer-induced attraction. The present simulations show that the non-pairwise additivity has a pronounced effect on the structure and phase diagram of a colloid-polymer mixture.

Unsere Computersimulationsuntersuchung umfaßt ein einfaches Modell eines Kolloids, das in einer verdünnten Polymerlösung dispergiert ist. Dazu bedienen wir uns eines erst kürzlich entwickelten Berechnungsschemas, das die direkte numerische Simulation bei konstantem osmotischen Druck des Polymeren ermöglicht. Wir berechnen die Interaktionen, die vom Polymer ausgehen, die lokale Struktur des Kolloids sowie das Phasendiagramm. Insbesondere wurde die vom Polymer ausgehende Anziehung, der Einfluß ihrer nicht paarweisen Additivität, untersucht. Die vorliegenden Simulationen ergeben, daß die nicht paarweise Additivität einen deutlichen Einfluß auf die Struktur und das Phasendiagramm von Kolloid-Polymer Gemischen hat.

1 Introduction

Dissolving non-adsorbing polymer in a colloidal dispersion gives rise to a change in the properties of the dispersion. The main effect is that, upon adding enough polymer, the colloidal particles tend to cluster [1, 2]. This is due to the fact that the presence of the polymers induces an attractive interaction between the colloidal particles. This polymer-induced attraction stems from the presence of depletion layers, i. e. regions with a depleted polymer concentration, around the colloidal particles. An important feature of the polymer-induced interaction is the fact that it is not pairwise additive.

The theoretical study of the structural and phase properties of colloid-polymer mixtures was initiated by Vrij [3]. He used a simple model, introduced earlier by Asakura and Oosawa [4] (hereafter referred to as the AO-model), to describe the system. In the AO-model the colloidal particles are represented by hard spheres, and the polymers by spheres that are mutually inter-penetrable and have an excluded-volume interaction with the colloidal hard spheres. Clearly, the AO-model

neglects the deformability of the polymer globules, and the interaction between the polymers. The work of Vrij has been extended by various authors who applied more advanced tools from the theory of liquids and solids to the AO-model [5, 6, 7, 8, 9]. There have been also a few studies of models where the polymers are represented by flexible chains (see e. g. [10]).

In most of the theoretical studies of the AO- and other models the polymer-induced interaction between the colloidal particles is approximated to be pair-wise additive. Only recently a study has been reported that takes into account the many-body part of the polymer-induced interaction in the AO-model, using scaled-particle theory [8, 9]. However, the theoretical models remain still too complex to be solved exactly. It is therefore desirable to know the "exact" properties of model colloid-polymer mixtures. These can be provided by computer simulation [11].

Numerical simulation of detailed microscopic models for colloids dispersed in a polymer solution requires orders of magnitude more computer time than similar simulations of models for atomic or simple molecular systems. The reason for this is twofold. Firstly, the relaxation times in mixtures are, in general, longer than in pure systems. Secondly, the relaxation times in polymeric systems are orders of magnitude longer than in atomic systems. Consequently, one has to perform longer simulations to sample a representative part of the phase space. Fortunately, many of the properties of colloid-polymer mixtures do not depend sensitively on the molecular details of the model. Here we present a simulation study of a simple model for colloid-polymer mixtures [11]. This model can be seen as an extension of the AO-model, with the ideal polymer spheres replaced by ideal lattice chains. Although this model is clearly too simple to be realistic, it includes the most essential elements: it takes into account the flexibility of the polymers and the non-pair-wise additivity of the polymer-induced interaction.

The results presented in this paper are an extension of earlier reported results [11]. For completeness, parts of these earlier results will be repeated here. This paper is organized as follows. First we will introduce the model, give expressions for the main thermodynamic quantities, and briefly discuss the numerical technique we used to simulate the model. Subsequently we present some results for the polymer-induced interaction, the local structure, and the phase diagram of the model colloid-polymer mixture.

2 Model and Thermodynamics

We consider the following model for a colloid dispersed in a polymer solution. The colloidal particles are represented by hard spheres with a diameter denoted by σ_{col} . The polymers are represented by ideal (non-self-avoiding) chains that are

* FOM Institute for Atomic and Molecular Physics, Kruislaan 407, 1098 SJ Amsterdam/The Netherlands.

confined to a cubic lattice. The length of the polymer, i. e. the number of connected lattice links that constitute the polymer, is denoted by l . If every occupied lattice site is associated with a polymer segment, an l -link lattice polymer has $l + 1$ segments. The solvent is not taken into account explicitly. Fig. 1 gives a schematic two-dimensional illustration of the model. In the following the lattice spacing will be used as the unit of

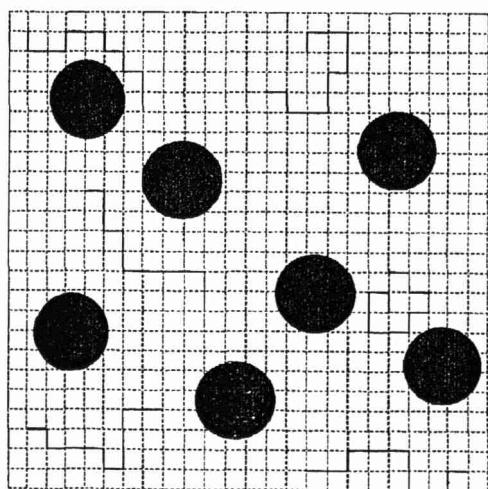


Fig. 1. Schematic two-dimensional illustration of a simple lattice model for a colloid-polymer mixture. The black circles indicate hard spheres that represent the colloidal particles. The thick lines on the lattice indicate the lattice chains that represent the polymer

length. The ideal polymers have an excluded-volume interaction with the colloidal hard spheres: the lattice sites occupied by the colloidal hard spheres are not accessible to the polymer segments. The lattice sites not occupied by the colloidal hard spheres can be occupied by all polymer segments with equal probability. In the following we will refer to this model as the lattice colloid-polymer model. Although quite simple, the model is expected to yield a fair description of a sub-class of systems studied experimentally (see e.g. [12, 13]). For example, the interaction between silica particles in an organic solvent is very close to a hard-sphere interaction. Dilute solutions of polymers in a theta-solvent are reasonably well modeled by non-interacting polymers.

The statistical mechanics of the lattice colloid-polymer model has been described in Ref. [11]. Here, we recall the main notions. Consider a system with N colloidal hard spheres in a volume V , in chemical equilibrium with a large reservoir of ideal lattice polymers with fugacity z . The fugacity is related to the polymer chemical potential μ by $z = e^\mu$, and is proportional to the osmotic pressure of the polymers. As all interactions are determined completely by excluded volume, there is no temperature dependence. In the following we will assume $k_B T = 1$, with k_B the Boltzmann constant. The configurational part of the (partial) grand-canonical partition function Ξ for the system is given by:

$$\Xi(N, z, V) = \int_V dr^N \exp(-U_{hs}(r^N) + z\Omega(r^N; V)), \quad (1)$$

where $\Omega(r^N; V)$ denotes the partition function of a single lattice polymer for a given colloid configuration r^N . $\Omega(r^N; V)$ is equal to the total number of possible polymer conformations. U_{hs} denotes the hard-sphere interaction potential between the colloidal particles. Equation (1) shows that the lattice colloid-

polymer model is equivalent to a single-component system with interaction potential U_{hs+pol} given by:

$$U_{hs+pol}(r^N; V) = U_{hs}(r^N) - z\Omega(r^N; V). \quad (2)$$

The one-polymer partition function $-z\Omega$ is identified as the polymer-induced interaction. For convenience we will express Ω in terms of number of excluded polymer conformations $\bar{\Omega}$:

$$\Omega(r^N; V) = \Omega^{id}(V) - \bar{\Omega}(r^N).$$

Here the ideal term, $\Omega^{id}(V)$, is defined as the number of conformations on an empty cubic lattice:

$$\Omega^{id}(V) = \frac{1}{2} V 6^l.$$

We can write $\bar{\Omega}(r^N)$ as a sum of one-, two-, three- and more-body contributions:

$$\bar{\Omega}(r^N) = \sum_{i=1}^N \bar{\Omega}^{1b}(r_i) + \sum_{\substack{\text{pairs} \\ i < j}}^N \bar{\Omega}^{2b}(r_{ij}) + \sum_{\substack{\text{triples} \\ i < j < k}}^N \bar{\Omega}^{3b}(r_{ij}, r_{ik}) + \dots, \quad (3)$$

with $r_{ij} = |r_j - r_i|$, where r_i denotes the coordinates of particle i . $\bar{\Omega}^{1b}$ is defined as the number of conformations excluded by one sphere. $-\bar{\Omega}^{2b}$ and $\bar{\Omega}^{3b}$ are defined as the number of conformations excluded simultaneously by two and three spheres, respectively. A schematic illustration is given in Fig. 2. The one-body contribution $\bar{\Omega}^{1b}$ is approximately constant, as it does not depend on the position of the colloidal particles, except for

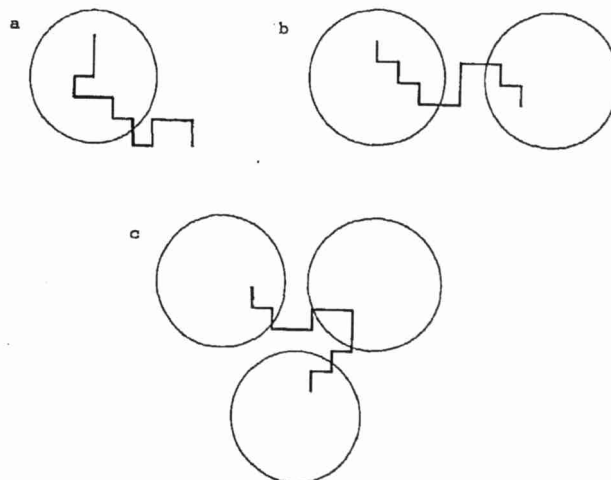


Fig. 2. One-, two- and three-body contributions to the number of excluded conformations $\bar{\Omega}$. The circles indicate the hard-sphere colloidal particles, whereas the lines represent the lattice chains. Figure (a) illustrates the one-body contribution $\bar{\Omega}^{1b}$. Figure (b) illustrates the two-body contribution $\bar{\Omega}^{2b}$, that corrects for the doubly counted conformations by the one-body contributions. Figure (c) illustrates the three-body contribution $\bar{\Omega}^{3b}$, correcting for the doubly counted conformations in the sum of the one- and two-body contributions

small variations due to the discreteness of the lattice. The two-body term $\bar{\Omega}^{2b}$ corrects for the double counted conformations in the one-body contribution, and provides an attractive contribution to the polymer-induced interaction $z\bar{\Omega}$. The three-body term $\bar{\Omega}^{3b}$ corrects for the double counted conformations in the sum of the one- and two-body contributions. It is a monotonically decreasing function of the inter-particle distances, and gives rise to a repulsive contribution to the polymer-induced interaction. If we neglect in the expansion of $\bar{\Omega}$ the

three- and more-body terms we obtain the two-body approximation to the polymer-induced interaction:

$$U_{hs+pol}^{2b}(\mathbf{r}^N; V) = \sum_{i < j} U_{hs}(r_{ij}) + z\bar{\Omega}^{2b}(r_{ij}). \quad (4)$$

As we can see from Fig. 2, for relatively short polymers U_{hs+pol}^{2b} is expected to be a good approximation for the full polymer-induced interaction U_{hs+pol} (2), as there will be no conformations intersecting with three or more colloidal spheres simultaneously. However, as we will show below, for longer polymers this does not hold.

Next, we turn to the thermodynamic properties of the colloid-polymer model. The thermodynamic potential F corresponding to the partition function Ξ (Eq. 1) is defined as:

$$F(N, z, V) = -\ln \Xi(N, z, V). \quad (5)$$

We will refer to F as the free energy of the colloid-polymer model. The pressure is defined by:

$$P = -\left(\frac{\partial F}{\partial V}\right)_{N, z}. \quad (6)$$

However, as Ω is in general a complicated function, that is not pair-wise additive in the inter-particle distances, the derivative with respect to V in Eq. (6) cannot be evaluated analytically. Therefore we will use thermodynamic integration to obtain an alternative expression for the pressure. To arrive at that expression we first write the free energy as:

$$F(N, z, V) = F(N, z = 0, V) + \int_0^z dz \left(\frac{\partial F}{\partial z}\right)_{N, V}. \quad (7)$$

Noting that $F(N, z = 0, V)$ is the free energy of a hard-sphere system, and using Eqs. (1) and (5) we arrive at the following expression for the free energy:

$$F(N, z, V) = F_{hs}(N, V) - \int_0^z dz \langle \Omega \rangle_{N, z, V}, \quad (8)$$

where F_{hs} denotes the free energy of the hard-sphere system. The brackets denote the ensemble average. Inserting this expression for the free energy in the definition of the pressure (6) we obtain:

$$P(\rho_{col}, z) = -\frac{\partial}{\partial V} \left(F_{hs}(N, V) - \int_0^z dz \langle \Omega \rangle_{N, z, V} \right) \\ = P_{hs}(\rho_{col}) + \int_0^z dz \frac{\partial \langle \Omega \rangle_{N, z, V}}{\partial V}, \quad (9)$$

where P_{hs} denotes the pressure of the hard-sphere system and $\rho_{col} (= N/v)$ is the colloid density. Hence, to obtain the pressure with thermodynamic integration, one has to compute the average one-polymer partition function $\langle \Omega \rangle$ as function of polymer fugacity z and colloid-density ρ_{col} . The chemical potential μ_{col} of the colloidal spheres is defined by

$$\mu_{col} = \frac{F + PV}{N}.$$

Inserting the relations for the free energy (8) and the pressure (9) yields the following expression for the chemical potential of the colloidal hard spheres:

$$\mu_{col}(\rho_{col}, z) = \mu_{hs}(\rho_{col}) - \frac{1}{N} \int_0^z dz \langle \Omega \rangle_{N, z, V} + \frac{1}{\rho_{col}} \int_0^z dz \frac{\partial \langle \Omega \rangle_{N, z, V}}{\partial V}, \quad (10)$$

where μ_{hs} denotes the chemical potential of the hard-sphere system.

Next we discuss briefly the numerical techniques. The one-polymer partition function Ω is given by the sum of all possible polymer conformations. Frenkel [14] has shown that this partition function can be computed using an efficient algorithm, similar to the "moment-propagation" method [15] developed in the context of simulations of lattice-gases. The "propagation" method is based on an iterative scheme. Starting from the partition function of a one-segment polymer, the partition function of a two-segment polymer is computed. This "propagation" step is repeated l times to arrive at the partition function of the $l + 1$ -segment polymer. Using this method it is also straightforward to compute the average polymer-segment density at each lattice site [16]. From a computational point of view the propagation method is highly attractive, as it is perfectly suited for processing on a vector- or parallel computer.

By combining the moment-propagation method to compute the one-polymer partition function Ω with the standard Monte Carlo techniques, it is straightforward to simulate the colloid-polymer model described as a one-component system with interaction potential $U_{hs}(\mathbf{r}^N) - z\Omega(\mathbf{r}^N; V)$ (Eq. (1)).

3 Results

The specific model we will consider in this work consists of hard-sphere colloidal particles with diameter $\sigma_{col} = 10.5$ and lattice chains with length $l = 10$ and $l = 50$. The "size" of the polymers, as measured by their radius-of-gyration R , relative to the size of the colloidal spheres is given by $2R_{l=10}/\sigma_{col} \sim 0.25$ and $2R_{l=50}/\sigma_{col} \sim 0.56$. In the Monte Carlo simulations periodic boundary conditions were used. The length of the cubic periodic box was taken to be an integer multiple of the lattice spacing, in order to match the periodic boundary conditions for the lattice. Each simulation consisted of 10,000–20,000 Monte Carlo cycles, after an initial equilibration of 2,000–5,000 cycles. Here one cycle consists of one attempted particle move for each particle in the system. We have studied systems with $N = 32$ –108 particles. In the following the polymer fugacity will be expressed in reduced units, and is denoted by z^* . Here z^* is defined by $z = z^* \times z_{id}$, with $z_{id} = 6^l$. The values for the colloid density will be given relative to hard-sphere regular closed packing, and are denoted by ρ^* . Below we will present some typical results for the two- and three-body polymer-induced interactions, the local structure, the equation-of-state, and the phase diagram.

3.1 Interactions

The two- and three-body contributions ($\bar{\Omega}^{2b}$ and $\bar{\Omega}^{3b}$ in Eq. (3)) give an attractive, respectively repulsive contribution to the polymer-induced interaction $z\bar{\Omega}$. In order to compute the two- and three-body contribution we considered a system with two and three colloidal hard spheres, respectively, at various mutual distances. The three spheres were put in an equilateral configuration. In Fig. 3 we have plotted normalized values of the two- and three-body contributions for the lattice colloid-polymer model (solid lines). For comparison we have also plotted the result for the corresponding AO-models (dotted lines) [3]. For the prescription of the mapping onto the corresponding AO-model see [16].

The attractive two-body contribution $\bar{\Omega}^{2b}$ compares reasonably well with the AO-model, except that the range of the interactions in the AO-model is slightly shorter. The absolute values agree within 10%. The shorter range in the AO-model must be attributed to the fact that there is a significant number of polymer conformations that have a spatial extent larger than the diameter of the polymer sphere in the AO-model. If

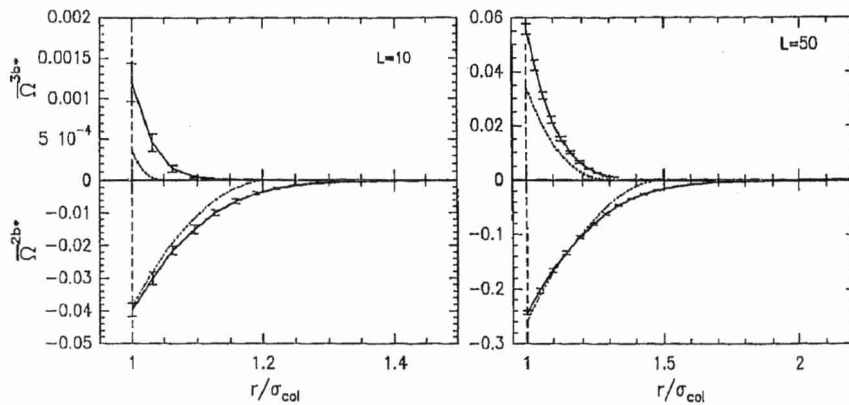


Fig. 3. Two- and three-body contribution to the polymer-induced interaction as function of the distance of the colloidal spheres with diameter $\sigma_{col} = 10.5$. The two figures show the results for two different polymer lengths, as indicated in the figures. The lower part of each figure shows the (normalized) two-body contribution $\bar{\Omega}^{2b}$, the upper part gives the results for the (normalized) three-body contributions $\bar{\Omega}^{3b}$. The solid lines show the results for the lattice colloid-polymer model; the dotted lines the results for the corresponding AO-model. The error-bars indicate the mean-square variation in the computed values, due to the finite lattice spacing

we look at the three-body contribution $\bar{\Omega}^{3b}$ we observe a rapid decrease with increasing colloidal-sphere distance. Here, the most important observation is the increase of the relative three-body contribution $\bar{\Omega}^{3b}/\bar{\Omega}^{2b}$ upon increasing polymer length. For $l = 10$ the three-body contribution $\bar{\Omega}^{3b}$ is almost negligible, whereas for the $l = 50$ it is a significant fraction of the two-body contribution $\bar{\Omega}^{2b}$. Obviously, the $l = 10$ polymers are too short to intersect with three spheres. From this we can conclude that only for these short polymers the two-body approximation (4) yields an accurate description of the polymer-induced interaction (2). In contrast to the comparison for the two-body contribution, the three-body contribution of the lattice colloid-polymer model differs significantly from the three-body contribution of the corresponding AO-model. Apparently, the conformations with a spatial extent larger than the diameter of the corresponding AO-polymer sphere, have an enhanced contribution to the three-body term.

3.2 Local colloid structure

We have studied the local structure of the colloid-polymer mixture with the long polymers ($l = 50$) by Monte Carlo simulation. In particular we investigated the effect of the many-body contributions to the polymer-induced interaction. We considered a system of $N = 108$ colloidal hard spheres at a colloid density $\rho^* = 0.56$, and a polymer fugacity $z^* = 0.01$.

In Fig. 4 we have plotted the radial distribution function $g(r)$ for the colloidal component in the mixture (solid lines). For comparison we also plotted the radial distribution function of a hard-sphere fluid at the same density (dotted lines). We observe a slight difference in the local structure of the mixture compared to the structure of the hard-sphere fluid. The polymer-induced attraction leads to an increase of $g(r)$ for r close to σ_{col} . In addition the second peak of $g(r)$ has also slightly changed.

In order to quantify the effect of the many-body part of the polymer-induced interaction, we performed simulations in which we replaced the full polymer-induced interaction (2) by the approximate two-body interaction, given by Eq. (4). The radial distribution function $g(r)$ obtained from this simulation is plotted as a dashed line in Fig. 4. Clearly, neglecting the three- and more-body contribution leads to a significant change in the radial distribution function. As we have seen above, the two-body approximation overestimates the polymer-induced attraction. This leads, in the "two-body" model, to a strong increase of the radial distribution function at values of r close to σ_{pol} . In addition the second peak of $g(r)$, in the "two-body" model, shows the onset of splitting, indicating a drastic, but spurious change in the local structure of the colloid.

3.3 Equation of state and phase diagram

There is experimental (see e. g. [12, 13, 10]) and theoretical (see e. g. [6, 7, 8, 9]) evidence that a colloid dispersed in a polymer solution exhibits disordered "gas"- and "fluid"-like phases and an ordered "solid"-like phase. One expects that for polymer fugacities z above a certain (critical) value, a colloidal fluid phase separates into a dilute gas phase and a dense liquid or solid phase. To illustrate that such a phase separation also might occur in the lattice colloid-polymer model considered in this chapter, we performed Monte Carlo simulations of this model at a colloid density $\rho^*_{col} = 0.25$, for a relatively "high" value ($z^* = 0.015$) of the polymer fugacity. The simulation started from an equilibrated hard-sphere configuration. Fig. 5 shows snapshots of the configuration of the colloidal spheres and the local polymer-segment concentration after several thousand Monte Carlo cycles. We see that there are distinct regions with low and high concentrations. This indicates that the colloid has phase separated into a low and a high density phase. Unfortunately, the exact location of the phase equilibria cannot be obtained directly from these kinds of Monte Carlo simulations due to large finite-size effects for these small system sizes.

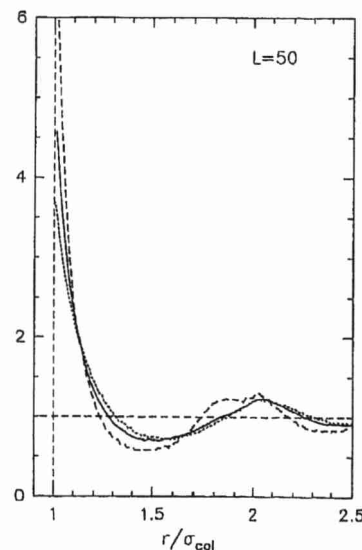


Fig. 4. Radial distribution function of hard-sphere colloids in a mixture with long ($l = 50$) polymers. The polymer fugacity is $z^* = 0.01$. The colloid density is 56% of regular close packing. The solid line indicates the results obtained with the full polymer-induced interaction (Eq. 2). The dashed line indicates the results obtained with an approximate two-body polymer-induced interaction (Eq. 4). The dotted line denotes the results for a hard-sphere fluid and serves as a reference

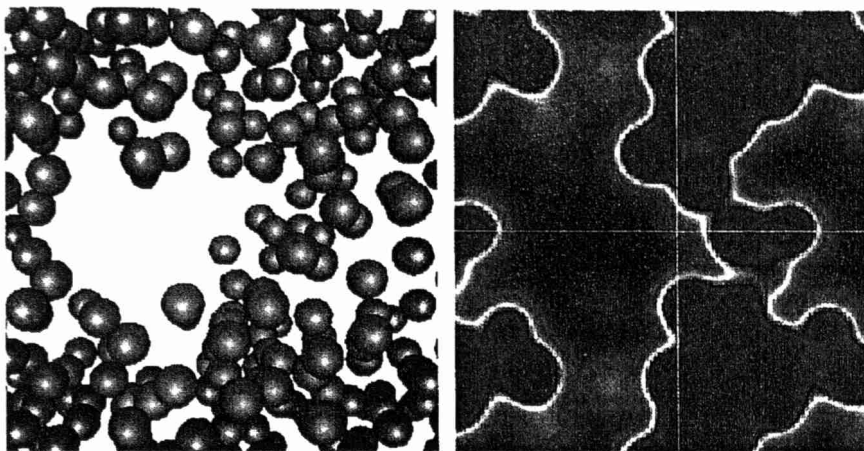


Fig. 5. Snapshot of a simulation of colloidal hard spheres dispersed in an ideal polymer solution at relatively high polymer fugacity ($z^* = 0.015$). The average reduced density of the colloidal hard spheres is $\rho_{col}^* = 0.25$. In the left figure the colloidal hard spheres are shown, where the purple spheres indicate periodic images of the blue spheres. In the right figure we have plotted the corresponding polymer-segment concentration in a thin slice in the plane of the page, cut through the system. The color-coding is red to blue, for high to low polymer-segment density, respectively. We observe that there are distinct regions with low and high concentrations. It indicates that the colloid has phase separated into a low- and a high-density phase, with a high and low polymer-segment concentration, respectively

In order to determine a phase coexistence we have to locate the two state points in both phases, that have equal pressure, equal polymer chemical potential, and equal chemical potential of the colloidal particles. The chemical potential of the polymers is imposed in the simulations. The pressure and chemical potential of the colloidal component is computed explicitly by thermodynamic integration, using Eqs. 9 and 10, where the pressure and chemical potential of the reference hard-sphere fluid and solid are obtained from literature [17, 18, 19]. The actual computation involved evaluating $\langle \Omega \rangle$ for several values of the fugacity z^* and the colloid density ρ^* by Monte Carlo simulation. The integration in the expressions for the pressure and the chemical potential was then performed numerically.

In Fig. 6 we show, as an illustration, the equation of state $P(\rho)$ of the colloid fluid phase at polymer fugacity $z^* = 0.0095$ ($l = 50$). We observe extrema, indicated by arrows, in the $P - \rho$ curve at low and high density. These extrema correspond to the spinodal points. In between these points there is no stable uniform fluid phase: the fluid has phase separated into a dilute gas phase and a dense liquid phase. The spinodal points do not constitute the exact location of the phase coexistence, as they do not have equal pressure and equal colloid chemical potential. We have determined the exact location of the possible fluid-solid, gas-liquid, and gas-solid phase coexistence numerically, for various values of the polymer fugacity. In Fig. 7 we have plotted the resulting phase diagram in the $\rho_{col}^* - z^*$ plane for polymers with length $l = 50$. Our computation indicates the existence of a colloidal fluid-solid, gas-liquid, and gas-solid

coexistence. The gas-liquid coexistence could not be computed in a small region around the critical value of the fugacity, i.e. the minimum polymer fugacity at which a phase separation occurs. This is due to the large statistical errors in the estimate for the chemical potential μ_{col} in the low-density gas phase, in this region.

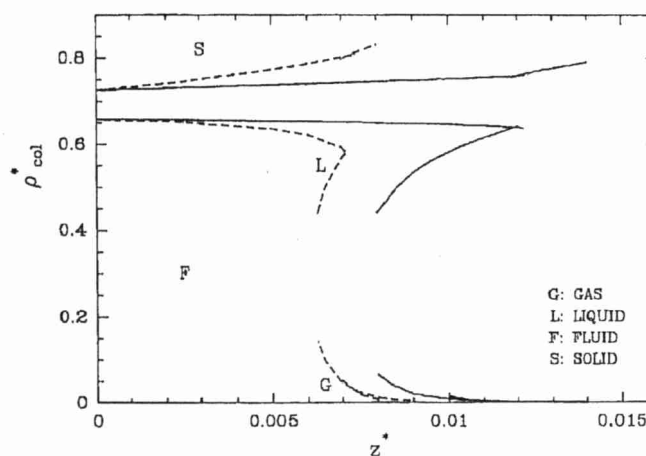


Fig. 7. Phase diagram of lattice colloid-polymer mixture of colloidal hard spheres of diameter $\sigma_{col} = 10.5$ and polymers of length $l = 50$. The solid lines denote the phase boundaries obtained by simulations of the model with the true many-body polymer-induced interaction (Eq. 2). The dashed lines represent the phase boundaries obtained with simulations of the model with the approximate two-body polymer-induced interaction (Eq. 4).

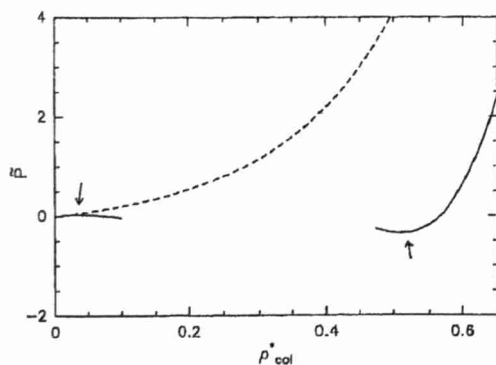


Fig. 6. Reduced pressure versus density in a colloid-polymer mixture with $l = 50$ -polymers and polymer fugacity $z^* = 0.0095$ (solid line). The dashed line indicates the hard-sphere result, and serves as a reference. The reduced pressure is defined as $P = (P - z^*)\sigma_{col}^3$. The arrows indicate the spinodal points

To quantify the effect of the many-body part of the polymer-induced interaction on the phase diagram, we performed simulations where we replaced the full polymer-induced interaction (2) by the approximate two-body interaction, given by Eq. (4). The equations of state and phase-equilibria were computed by thermodynamic integration using Eqs. (9) and (10). The resulting phase diagram is compared with the one obtained with the full polymer-induced interaction in Fig. 7. Clearly there is a significant difference. We observe a lower value of the critical fugacity for the "two-body" model. Furthermore we see that for the "two-body" model there is an enhanced density change at the fluid-solid coexistence line. Apparently the two-body approximation underestimates the stabilization of the liquid state. This must be attributed to the fact that the two-body polymer-induced interaction overestimates the attractive part of the polymer-in-

duced attraction. Apparently, a deeper attractive tail added to a hard-core repulsion favors a solid-, or dilute gas phase over a dense liquid phase.

4 Discussion

We have used computer simulations to study a simple model for colloids (hard spheres) dispersed in a dilute polymer (ideal lattice chains) solution. We find that, for all but the shortest polymers, the full polymer-induced interaction can not be described by a sum of two-body contributions: the two-body interaction strongly overestimates the polymer-induced attraction. Our simulations of the polymer-colloid mixture show that the true many-body interactions have clearly observable consequences. First of all, the local structure of the colloid, as measured by the radial distribution function, computed with the true many-body polymer-induced interaction, differs considerably from the results obtained with the approximate two-body interaction. Secondly, we have computed the phase diagram for the colloid-polymer mixture and compared it with the phase diagram for the "two-body" model. We find that the strong overestimation of the polymer-induced attraction in the "two-body" model leads to a gas-liquid phase separation of the colloid at significantly smaller values of the polymer fugacity, than is observed in the full colloid-polymer model. The simulation results suggest that the assumption of pair-wise additivity of the polymer-induced interaction, used in most of the theoretical descriptions, is an oversimplification.

Acknowledgements

We thank A. Vrij and H. Lekkerkerker for useful discussions and suggestions. This work is part of the research program of the Stichting voor Fundamenteel Onderzoek der Materie (Foundation for Fundamental Research of Matter) and was made possible by financial support from the Nederlandse Organisatie voor Wetenschappelijk Onderzoek (Netherlands Organisation for the Advancement of Research), and the Dutch Ministry of Economic Affairs within the framework of the Innovatief Onderzoekprogramma Polymeercomposieten en Bijzondere Polymeren (Innovative Research Program Polymer-Composites and Special Polymers). Computer time on the CRAY-YMP at SARA, was

made available through support of the Stichting Nationale Computer Faciliteiten (Foundation for National Computing Facilities).

Bibliography

1. Monaghan, B. R. and White, H. L.: J. Gen. Physiol. 19 (1935) 715.
2. Bondy, C.: Trans. Faraday Soc. 35 (1939) 1093.
3. Vrij, A.: Pure Appl. Chem. 48 (1976) 471.
4. Asakura, S. and Oosawa, F.: J. Chem. Phys. 22 (1954) 1255.
5. Hall, A. P.; Gast, C. K. and Russel, W. B.: J. Colloid Interface Sci. 96 (1983) 251.
6. Gast, A. P.; Russel, W. B. and Hall, C. K.: J. Colloid Interface Sci. 1 (1986) 161.
7. Canessa, E.; Grimson, M. J. and Silbert, M.: Mol. Phys. 67 (1989) 1153.
8. Lekkerkerker, H. N. W.: Coll. and Surf. 51 (1991) 419.
9. Lekkerkerker, H. N. W.; Poon, W. C.-K.; Pusey, P. N.; Stroobants, A. and Warren, P. B.: Europhys. Lett. 20 (1992) 559.
10. Vincent, B.; Edwards, J.; Emmett, S. and Groot, R.: Colloids Surfaces 31 (1988) 267.
11. Meijer, E. J. and Frenkel, D.: Phys. Rev. Lett. 67 (1991) 1110.
12. de Hek, H. and Vrij, A.: J. Colloid Interface Sci. 70 (1979) 592.
13. de Hek, H. and Vrij, A.: J. Colloid Interface Sci. 84 (1981) 409.
14. Frenkel, D.: J. Phys.: Condens. Matter 2 (1990) SA 265.
15. Frenkel, D. and Ernst, M. H.: Phys. Rev. Lett. 63 (1989) 2165.
16. Meijer, E. J.: Ph. D. thesis, FOM-Institute AMOLF/University of Utrecht, 1993.
17. Carnahan, N. F. and Starling, K. E.: J. Chem. Phys. 51 (1969) 635.
18. Hoover, W. G. and Ree, F. H.: J. Chem. Phys. 49 (1968) 3609.
19. Hall, K. R.: J. Chem. Phys. 57 (1972) 2252.

The authors of this paper

Evert Jan Meijer studied physics at the University of Utrecht. Since 1988 he works at the FOM-Institute for Atomic and Molecular Physics in Amsterdam. In 1993 he obtained his Ph. D. in the field of computer simulation of many-particle systems. His scientific interest concerns the numerical study of the structural properties and phase equilibria of complex systems, such as colloidal dispersions and molecular solids.

Daan Frenkel studied Physical Chemistry at the University of Amsterdam. In 1977 he obtained his Ph. D. on a combined experimental/numerical study of quantized rotation in fluids. Until 1980 he worked as a post-doc in Los Angeles (UCLA). Subsequently he worked at Shell Research in Amsterdam and at the Physics Department of the University of Utrecht. In 1987 he started a computer-physics group at the FOM-Institute for Atomic and Molecular Physics in Amsterdam. He is also associated with the Van 't Hoff Laboratory of the University of Utrecht.

11447

Neues Schichtdicken-Meßgerät

Polytec wird auf der „Laser '93“ in München ein neues, optisches Schichtdickenmeßsystem vorstellen. Es arbeitet auf der Basis eines faseroptischen Diodenarray-Spektralphotometers. Das Meßverfahren ist sehr schnell und vollständig berührungslos. Über einen großen Meßbereich werden mehrere Messungen pro Sekunde durchgeführt und Schichten bis über 100 µm Dicke bestimmt. Die Schnelligkeit der Messung und die große Flexibilität durch die Verwendung von faseroptischen Sensoren ermöglicht auch die Schichtdickenbestimmung direkt in der Produktion. Die primären Anwendungsbereiche liegen in der Bestimmung von

- transparenten Folien
- beschichteten Folien

- dünnen optischen Schichten auf Brillengläsern, Filtergläsern etc.
- der Oberflächenqualität beschichteter Fenstergläser oder Scheinwerferreflektoren

Das Meßprinzip basiert auf der spektroskopischen Analyse von optischer Interferenz an dünnen Schichten. Durch simultane Erfassung eines kompletten Spektrums mit bis zu 1024 Datenpunkten erzielt man eine extrem hohe Genauigkeit. Gleichzeitig erhält man auch noch Informationen über die Reflexions- und Transmissionseigenschaften der untersuchten Materialien, z.B. die Farbart oder die Filtercharakteristik. Benutzerfreundliche Software erleichtert die Bedienung des Gerätes sowohl im Labor als auch im Prozeß.

31792